Int. J. Electrochem. Sci., 17 **(2022)** Article Number: 22103, doi: 10.20964/2022.19.16.

International Journal of
ELECTROCHEMICAL
SCIENCE
www.electrochemsci.org

Short Communication

Electrochemical Study of the Inhibition of Corrosion of HSn70-1 Tin Brass by Benzotriazole in $NaNO_2$ Solutions

Kewei Fang[*], *Hongqun Liu, Li Wang, Kunjie Luo and Chengtao Li*

Suzhou Nuclear Power Research Institute, Suzhou 215004, China
[*]E-mail: fangkewei@cgnpc.com.cn

Received: 16 March 2022 / *Accepted:* 9 May 2022 / *Published:* 10 September 2022

The purpose of this research was to see how the addition of Benzotriazole (BTA) in a $NaNO_2$ solutions affected the corrosion inhibition behavior of HSn70-1 tin brass. The open-circuit potential (OCP), polarization curve, and electrochemical impedance spectrum (EIS) of HSn70-1 Tin Brass were investigated using electrochemical methods using a $NaNO_2$ solutions containing 700 ppm $NaNO_2$ mass fraction and 0-20 ppm BTA mass fraction as the study system. The OCP of HSn70-1 tin brass in $NaNO_2$ solutions with BTA mass fractions of 0-20 ppm gradually shifted positively; as the BTA mass fraction increased, the charge transfer resistance of HSn70-1 tin brass increased, then decreased, and the self-corrosion current density decreased, then increased. The addition of BTA to $NaNO_2$ solutions can block the corrosion of HSn70-1 tin brass; the mass fraction of BTA is 0-20 ppm, and the corrosion resistance of HSn70-1 tin brass displays a trend of increasing and then decreasing as the BTA concentration in the system increases.

Keywords: HSn70-1 tin brass; Benzotriazole; Corrosion Inhibition; Electrochemical behaviors

1. INTRODUCTION

Power plants equipment cooling water system in the radiator generally uses copper and/or copper alloy tube [1-3], and its connected pipes, pumps, valves and other equipment are mostly made of iron-based materials [4-6]. To prevent the corrosion of iron-based materials, the general system must add a certain concentration of corrosion inhibitors, such as sodium nitrite [7], trisodium phosphate [8], and others, to improve the pH of the solution or react with the system materials to form an oxide film on the material's surface [9,10]. However, because copper and copper alloys are the cathode components in the system, these corrosion inhibitors have no obvious corrosion inhibition effect on them [11], making it necessary to use benzole as a corrosion inhibitoe.

Benzotriazole (BTA) corrosion inhibitor, which contains $NaNO_2$, NaOH, and BTA, is a frequently used corrosion inhibitor in cooling water systems [12]. Among them, $NaNO_2$ has oxidizing

properties, and the system material reacts in the material surface to form an oxide film, inhibiting corrosion of materials [13]. NaOH is used to control the pH of the system to reduce material corrosion [14], and BTA is used to inhibit corrosion of copper and/or copper alloys [15]. It is effectively preventing the corrosion of copper under stationary as well as dynamic conditions. Tin brass is not the corrosion-resistant meterial in many environments, especially in the radiator heat and cold exchange environment in long-term service. Tin brass tubes in contact with coolant contact is unreplaceable or difficulty replaceable componentsd, so we need to use corrosion inhibitors added into these environmental media to address any potential corrosion problems. This is a safety factor that is often utilized in the corrosion and protection of metals.

A. Bellaouchou [16] investigated the inhibit efficiency of BTA on the corrosion of 904L stainless steel (SS) in phosphoric acid, and found that BTA has a great influence on both anodic and cathodic processe of corrosion. The corrosion rate dropped and the inhibition efficacy improved as BTA concentration increased, and the inhibition was linked to BTA chemisorption on the surface of the 904L SS. G.K. Gomma [17,18] investigated the effect of BTA on the electrochemical properties of steel in H_2SO_4 solution and discovered that the passivation current, corrosion potential, passive potential, and polarization resistance of steel in 1 M H_2SO_4 increaseed with the increasing of BTA concentration. Whereas, the corrosion current density of steel increases with scan rate, which is due to an increase in passive potential. The inhibitor effect of BTA on corrosion of carbon steel was investigated, and showed that BTA hindered the anodic process of carbon steel corrosion. Its inhibitor efficacy increased with the increasing of BTA concentration, but when the inhibitory concentration exceeding the critical value, there was an adverse effect on corrosion of carbon steel. S.M. Milić [19] investigated the corrosion of BTA on copper in a variety of chloride ion solutions. Cu^+ was created on the copper surface at lower potentials, while Cu^{2+} generated primarily at higher potentials. Because of the production of [Cu(I)BTA], BTA had an inhibitor effect at low concentrations. While, at high concentrations, this molecule had an activating effect on dissolution of copper. S. Mamaş [20] and H.C. Shih [21] examined the corrosion mechanism of BTA on the corrosion of 70/30 brass in 0.1 M NaCl solution, and the results indicated that BTA act as an effective anodic corrosion inhibitor. In this solution Zn-BTA complex may generated on the surface of brass, which inhibits the corrosion of brass.

Presenrly, the published results about the effect of BTA on copper and/or copper alloys mostly focused on the near-neutral and slightly alkaline solution system [15,19-21], and few publications on the effect of BTA on corrosion characteristics of copper and/or copper alloys in the nitrite solution system [13,22]. Using $NaNO_2$ solutions as the base system and HSn70-1 Tin Brass as the test object, the effect of BTA concentration on the corrosion behavior of HSn70-1 Tin Brass in $NaNO_2$ solutions was investigated using electrochemical technique, such as open-circuit potential (OCP), electrochemical impedance spectrum (EIS), and potentiodynamic polarization tests.

2. MATERIALS AND EXPERIMENTAL PROCEDURES

2.1. Testing material

The chemical compositions of HSn70-1 tin brass is Cu 69.82%, Sn 1.02%,As 0.053%,Fe 0.005%, Pb0.002%, Sb, 0.003% Bi, 0.002% P0.005% and Zn Bal. The samples were cut into

dimension of 1cm×1cm×3mm. The copper wire is soldered and sealed with epoxy resin with the working surface of 1cm^2. Before the test, the working surface was polished down to 2000# SiC sandpaper in turn, ultrasonic washed using ethanol for 10 minutes, and quickly dried with cold air.

2.2. Testing solutions

The test solutions were $NaNO_2$, NaOH, and BTA, with a mass fraction of 700 ppm for $NaNO_2$. And the concentration of BTA in the test solutions were 0 ppm, 1 ppm, 5 ppm, 10 ppm, and 20 ppm. Meanwhile, the pH of the test solution medium was adjusted to 9.27 using 1 mol/L NaOH solution. All of these experiments were carried out at a temperature of 25±2 ºC.

2.3. Electrochemical tests and Surface morphology observation

A CS350 (Wuhan Corrtest Instruments Corp., Ltd.) electrochemical workstation with a standard three-electrode system, with a saturated calomel electrode (SCE) as the reference electrode, a platinum electrode serving as the auxiliary electrode, and an HSn70-1 tin brass serving as the working electrode. The open-circuit potential of HSn70-1 tin brass was continually measured. The potentiodynamic polarization measurements were performed from -500 mV below OCP to 500 mV_{SCE} at a scanning rate of 20 mV/min. EIS test was conducted after the OCP attaind stable. EIS was measured using an AC excitation signal of 10 mV in the frequency range of 100-0.01 kHz, and the obtained data were fitted using ZsimpWin 3.5 software. After that, a dynamic potential scan was performed.

The specimens were analyzed and characterized after corrosion using scanning electron microscopy (SEM, XL30-FEG ESEM) to observe the corrosion morphology of HSn70-1 tin brass after 672 hours in $NaNO_2$ solution and then 308 hours in $NaNO_2$ solution with different concentration of BTA.

3. RESULTS AND DISCUSSION

3.1. Open-circuit potential test

The OCP of HSn70-1 tin brass in $NaNO_2$ solutions containing various concentration of BTA from 0 ppm to 20 ppm is shown in Fig. 1. With the increase of the BTA concentration in $NaNO_2$ solutions, the OCP curves of HSn70-1 tin brass shifted to positive direction, as shown in Fig. 1. In the presence of BTA in the system, the OCP values changed in the positive direction, which might be owing to the adsorbsion BTA molecules on the active sites on the surface of HSn70-1 tin brass and combined with the active copper, precipitating insoluble Cu-BTA complexes at the solution interface [20, 23]. Thus inhibiting the corrosion of HSn70 -1 tin brass, and the rate of film formation was faster at the early stage of immersion. The unadded HSn70-1 tin brass had the lowest corrosion potential of roughly -115 mV. When tha concentration of BTA increased to 20 ppm, the stable OCP of HSn70-1 tin brass is roughly 28 mV.

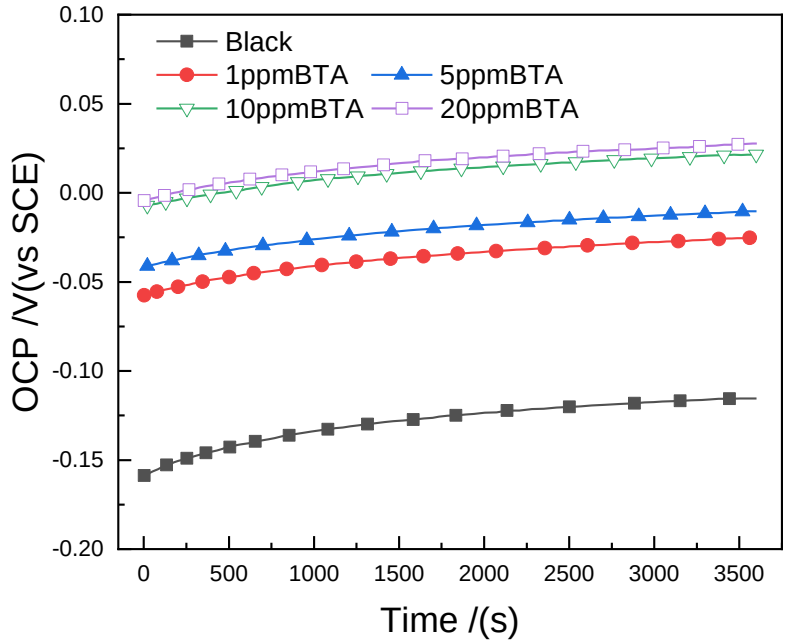

Figure 1. OCP of HSn70-1 tin brass in 700ppm $NaNO_2$ with different concentrations of BTA

3.2. Potentiodynamic polarization test

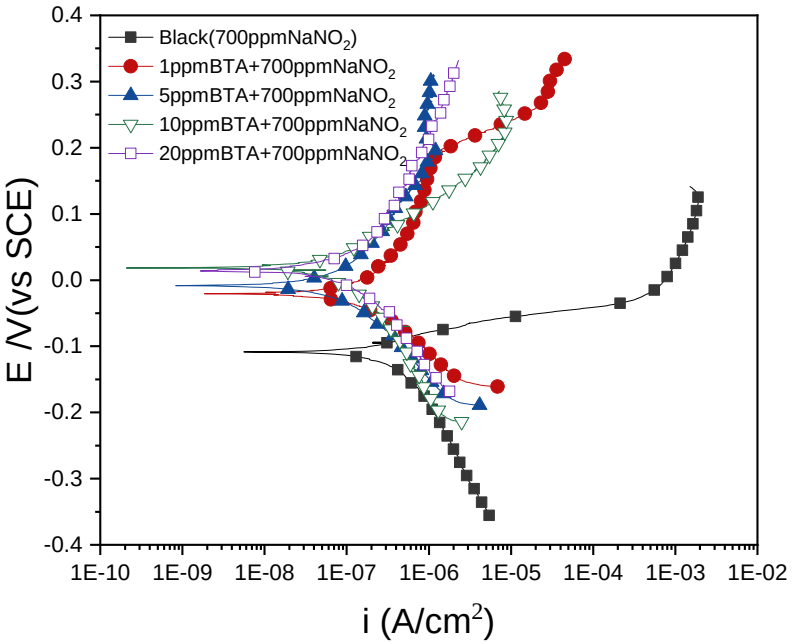

Figure 2. Potentiodynamic polarization curves of HSn70-1 tin brass in 700ppm $NaNO_2$ with different concentrations of BTA

As corrosion inhibitor concentration rises, the polarization curves gradually shift to the upper left, as seen in Figure 2. The cathodic and anodic differences of the polarization curves were obvious in comparison to the uncontrolled anodic curve. The addition of BTA primarily altered the anodic curve, transition platform area emerges in the anodic curve of the samples in the inhibited 700ppm $NaNO_2$ solution containing BTA, a phenomenon caused by inhibition [24].

The corrosion currents (i_{corr}), corrosion potential (E_{corr}), and β_a and β_b are the cathodic and anodic slope, obtained from potentiodynamic polarization curves in Fig. 2 are listed in Table 1. The E_{corr} of HSn70-1 tin brass in blank solution is -110 mV_{SCE}. The competing adsorption of NO_2^- and other anions (OH^-, etc.) in solution would alter its involvement in corrosion [25]. Furthermore, at this potential gap, NO_2^- can undertake oxidation processes. Cu^{2+} may have a catalytic function in NO_2^- oxidation, as evidenced by the stimulation of NO_2^- oxidation and the acceleration of the corrosion process over time [26], a notion supported by published research [27, 28]. However, as the inhibitor concentration increased, the corrosion potential of all of these samples shifs to a more positive position. The value of i_{corr} decreased with the increasing of BTA concentration and reaches the minimum value of 0.026 $\mu A \cdot cm^{-2}$ when the BTA concentration is 10ppm. When the BTA concentration is 20ppm, the i_{corr} increased from 0.026 $\mu A \cdot cm^{-2}$ to 0.330 $\mu A \cdot cm^{-2}$. Meanwhile, With the addition of BTA,The influence of the concentration BTA on β_a is more significant than β_b, indicating that the electrochemical behavior was controlled by the anodic reaction [29]. BTA is reported to be adsorbed on the surface of copper and copper oxides to form a protective film at low BTA concentrations [30]. However, at high BTA concentrations, especially in the presence of oxygen or other oxidants such as NO_2^- in the environment [23], the above adsorption is inhibited [20], which could explain the elevated corrosion current at 20 ppm BTA.

Table 1. Potentiodynamic polarization curve parameters for HSn70-1 tin brass in Fig. 2

C (ppm)	E_{corr} (mV/SCE)	i_{corr} ($\mu A \cdot cm^{-2}$)	β_a ($mV \cdot dec^{-1}$)	β_b ($mV \cdot dec^{-1}$)
0	-110	0.401	56	534
1	-21	0.385	473	332
5	-8	0.137	370	347
10	19	0.026	246	337
20	23	0.330	462	444

Table 1 further demonstrates that when the BTA concentration climbed from 0 to 20 ppm, E_{corr} increased progressively, with the shift being more evident at low concentrations. E_{corr} tended to remain steady when the BTA concentration was raised to 10 ppm, and when TBA was added, E_{corr} had minimal influence. When the BTA concentration was 10 ppm, the i_{corr} was the lowest, which is 93% lower than that in blank solution. When the BTA concentration was raised to 20 ppm, the icorr climbed again, climbing 11.7 times.

Corrosion inhibition efficiency (η) is an essential factor to evalate the inhibitor's corrosion prevention capacity. Eq. 1 was used to calculate the values of samples under settings with varying inhibitor concentrations [31]:

$$\eta\% = \frac{i_{corr}^0 - i_{corr}}{i_{corr}^0} \times 100\% \quad (1)$$

where i_{corr}^0 is the corrosion current density of HSn70-1 tin brass in the corrosion condition without inhibitor, and i_{corr}^0 is the corrosion current density of HSn70-1 tin brass in the corrosion condition with inhibitor.

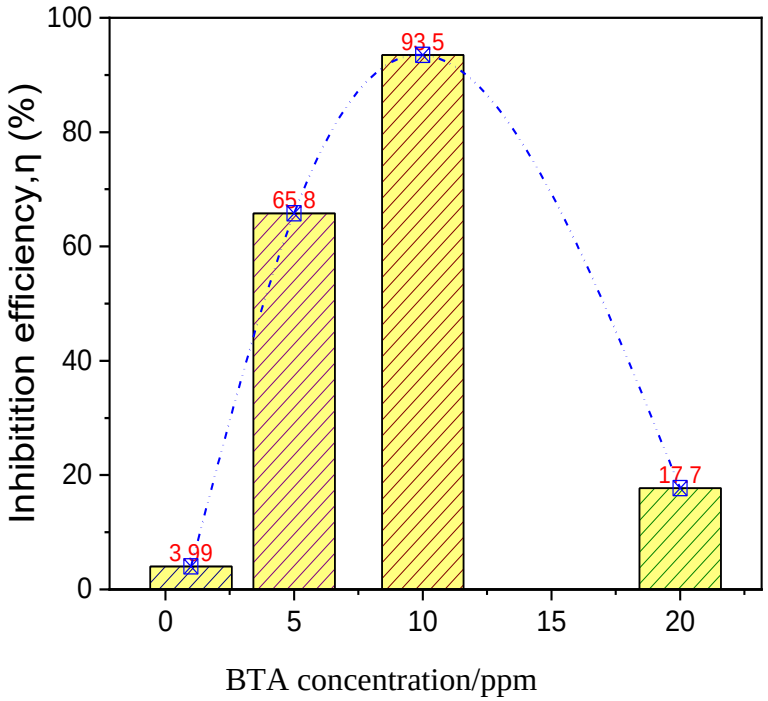

Figure 3. Corrosion inhibition efficiency of HSn70-1 tin brass in 700ppm $NaNO_2$ with different concentrations of BTA

The η of HSn70-1 tin brass in BTA solution with various concentrations of BTA is shown in Figure 3. The calculated η values rises and subsequently falls with BTA concentration, with the higest corrosion inhibition effectiveness of 93.5% when the concentration BTA is 10 ppm, indicating strong corrosion inhibition ability in $NaNO_2$ solutions.

3.3. Electrochemical impedance spectroscopy test

The EIS of HSn70-1 tin brass in 700 ppm $NaNO_2$ solutions with BTA mass fractions of 0 to 20 ppm is shown in Figure 4. The plots of HSn70-1 can be described as a capacitive arc representing the charge transfer resistance and the resistive relaxation process. The conentrcation of BTA did not modify the form of the impedance spectrum, but the radius of impedance rose dramatically with the addition of BTA, implying a difference in the magnitude of their polarization resistances. The magnitude of impedance radius is related to the corrosion resistance of materials, and when the concentration of BTA is 10 ppm, the radius of impedance is the largest and its polarization resistance value is the largest.

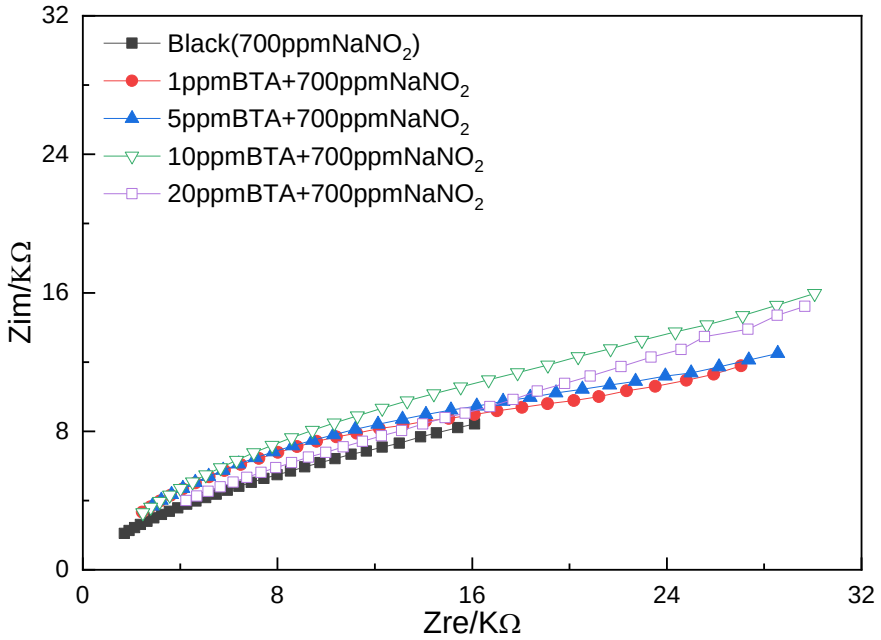

Figure 4. EIS of HSn70-1 tin brass in 700ppm $NaNO_2$ with different concentrations of BTA

The impedance spectrum was fitted using the equivalent circuit diagram shown in Figure 5, and the fitting results are shown in Table 2.

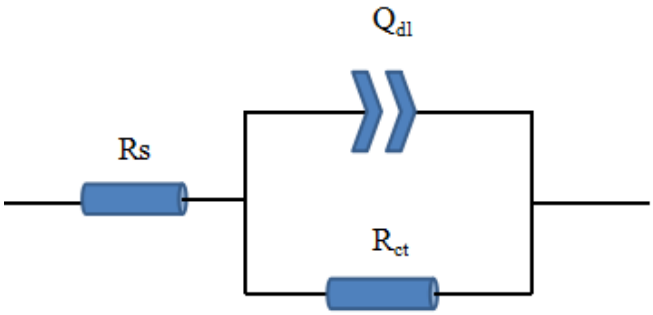

Figure 5. Circuit used to fitting the EIS curves in Figure 4.

In the analogous circuit, the capacitor (C) is replaced by the constant phase element (CPE) Q_{dl} [32] due to the surface heterogeneity induced by the corrosion process [33-35]. The microscopic roughness, which leads to a non-uniform distribution of solution resistance and double-layer capacitance, is the most frequently accepted explanation for the occurrence of CPE behavior and a depressed semicircle on the solid electrode [36]. In which, R_s is the solution impedance, R_{ct} is the resistance of the corrosion product film, Q_{dl} is the capacitance of CPE, C_{dl} denotes the bilayer capacitance, and n is the deviation parameter.

The following equation is used to compute the value of C_{dl} [37]:

$$C_{dl}=(Q_{dl}\cdot R_{ct}^{1-n})^{1/n} \quad (2)$$

When the BTA mass fraction in 700 ppm $NaNO_2$ solution is 0-20 ppm, the charge transfer resistance R_{ct} displays two distinct patterns with increasing BTA mass fraction, as shown in Table 2. R_{ct} steadily increases with increasing BTA concentration in the range of 0 to 10 ppm, from 194.32 kΩ·cm^2 to

466.10 kΩ·cm^2. R_{ct} progressively falls with rising BTA concentration in the 10-20 ppm range, eventually dropping to 338.00 kΩ·cm^2. C_{dl}, on the other hand, exhibits a declining and then growing tendency. When there was no BTA in the 700ppm $NaNO_2$ solution, C_{dl} was highest at 102.46 μF·cm^{-2}, lowest at 52.82 μF·cm^{-2} when the mass fraction was increased to 10 ppm, and C_{dl} steadily increased when the BTA content was increased. Because the adsorption of BTA resulted in a rise in the electric double layer thickness and a drop in the local dielectric constant, the decrease in C_{dl} suggested that the material's corrosion was repressed [38].

Table 2. Fitting results of impedance spectrum data of HSn70-1 tin brass

C (ppm)	$\boldsymbol{R}_s$ /Ω·cm^{-2}	$\boldsymbol{R}_{ct}$ /kΩ·cm^2	$\boldsymbol{Q}_{dl}$ /μF·cm^2·s^{n-1}	$\boldsymbol{C}_{dl}$ /μF·cm^{-2}	***n***
0	53.97	194.32	73.72	102.46	0.89
1	41.75	244.20	61.71	84.29	0.90
5	42.52	307.40	53.98	67.73	0.91
10	42.88	466.10	42.93	52.82	0.94
20	42.23	338.00	51.53	66.15	0.92

Table 2 demonstrates that when the mass fraction of BTA in 700ppm $NaNO_2$ solution is between 0 and 20 ppm, the corrosion resistance of HSn70-1 tin brass exhibits a trend of growing and subsequently decreasing with increasing BTA concentration in the system, which is compatible with the polarization curve fitting results.

When the mass concentration of BTA is low, the adsorption film formed on the metal surface is incomplete; as the concentration rises, the adsorption film becomes dense and complete, enhancing the corrosion inhibition effect and lowering the corrosion rate; however, as the BAT content rises, micelles can form, destroying the protective film on the metal surface and lowering the corrosion inhibition effect; when the BAT content rises, micelles can form, destroying the protective film on the metal surface and lowering the corrosion [39]. As a result, when the mass fraction of BTA in the system exceeds 10 ppm, the corrosion resistance of HSn70-1 tin brass falls as the concentration of BTA in the system rises.

3.4. Surface Morphology analysis

The following studies were designed to investigate the changes in the corrosion oxide coating of HSn70-1 tin brass after the addition of BAT to the sodium nitrite system corrosion inhibitor: To begin, HSn70-1 was pegged and corroded in 700 ppm $NaNO_2$ solution for 672 hours to generate a stable oxide coating, and then submerged in 700 ppm $NaNO_2$ solution for 308 hours with three concentrations of 1 ppm BTA, 10 ppm BTA, and 20 ppm BTA. With a magnification of ×5000, the SEM picture of the examined specimen surface is displayed in Fig. 6.

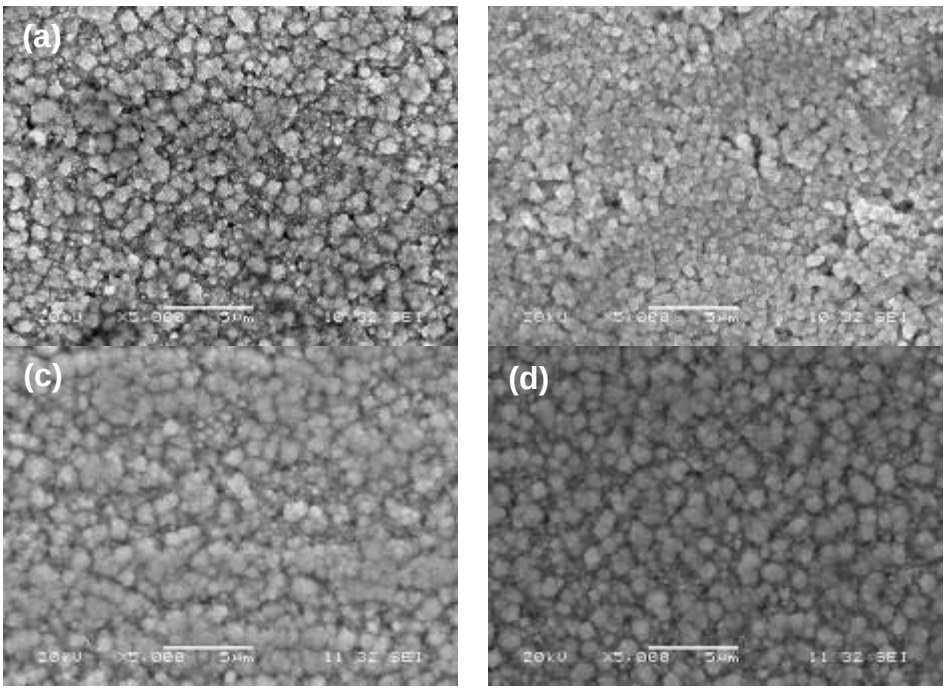

Figure 6. Corrosion morphologies of HSn70-1 tin brass after 672 hours of immersion in 700 ppm $NaNO_2$ solution, followed by 308 hours of immersion in BTA with various mass fractions.: (a) 0ppm; (b) 1ppm; (c) 10ppm; (d) 20ppm

The oxide film on the surface of the specimen appeared to be relatively loose after immersion in 700ppm $NaNO_2$ solution for 672 hours, with obvious protruding particles. When soaked in 1ppm BTA, 10ppm BTA, and 20ppm BTA solutions for 308 hours, the size of corrosion product particles on the surface of the specimen became uniform in 1ppm BTA solution, but still porous locally. in 10ppm BTA solution soaked specimens, corrosion oxide film became dense, verify the protective effect of BTA on the specimen [40]. In Figure 6 a, specimens oxide film granular some deficiency, said to be the original protective film occurred partly dissolved [41]. When the presence of BTA in the sodium nitrite solution system is compared to the surface morphology before the addition of BTA, there is an inhibitory effect on the corrosion of tin brass, with the best content at 10 ppm, which also provides visual evidence for the results of electrochemical testing.

4. CONCLUSION

In this paper, the electrochemical reponse of HSn70-1 tin brass in 700 ppm $NaNO_2$ solution with different concentrations of BTA between 0-20 ppm were tested, The following conclusions were drawn.

(1) The presence of BTA in the 700 ppm $NaNO_2$ solution system can form a protective film layer on the surface of HSn70-1 and inhibit the anodic disolution of HSn70-1, which in turn inhibits HSn70-1 corrosion.

(2) When the mass fraction of BTA increased from 0 ppm to 10 ppm, the charge transfer resistance of HSn70-1 increased and then reduced, while the corrosion current density and corrosion

rate fell and then increased. When the mass fraction of BTA in $NaNO_2$ solution was 10-20ppm, the corrosion resistance of HSn70-1 increased, then declined, as the BTA concentration was increased.

(3) In the cooling water system of power plant equipment, the corrosion resistance of HSn70-1 may be maintained by managing the range of BTA concentration to extend the service life of radiator tin brass tubes, given that the concentration of BTA would progressively decay.

ACKNOWLEDGMENTS
The authors would like to thank the National Key Research and Development Program of China (No. 2016YFB0700404) and Natural Science Foundation of China (No. 51375182) for their financial support.

References

1. N. Rajashekar Reddy, P. Abhilash and M. Rahul, *Mater. Today:. Proc.*, 39 (2021) 643
2. L. Huaqi, O. Zeyu, T. Xiaoyan, G. Li, L. Da, K. Xiaoya and S. Jianqiang, *Prog. Nucl. Energy.*, 146 (2022) 104145
3. M.L.C.M. Henckens and E. Worrell, *J. Cleaner Prod.*, 264 (2020) 121460
4. W. He, J. Zhang, H. Li, S. Liu, Y. Wang, B. Lv and J. Wei, *Appl. Therm. Eng.,* 207 (2022) 118176
5. W. Bengang, H. Hua, L. Honglei, W. Nannan and D. Mingqiu, *Energy Procedia.,* 100 (2016) 556
6. N.A. Pambudi, A. Sarifudin, R.A. Firdaus, D.K. Ulfa, I.M. Gandidi and R. Romadhon, *Alexandria Eng. J.,* 61(12) (2022) 9509
7. F. Bolzoni, A. Brenna and M. Ormellese, *Cem. Concr. Res.;* 154 (2022) 106719
8. M. Chen, L. Lin, Y. Zhang, S. Wu, E. Liu, K. Wang, J. Wang and J. Gong, *Particuology.,* 27 (2016) 115
9. J.K. Das and B. Pradhan, *J. Build. Eng*., 50 (2022) 104192
10. H. Kumar, R. Kumari, A. Yadav, R. Sharma and T. Dhanda, *Chem. Data Collect.,* 30 (2020) 100575
11. K. Higuchi, I. Shohji, T. Ando, S. Koyama, Y. Mizutani and Y. Inoue, *Procedia Eng.*, 184 (2017) 743
12. A. Chirkunov and Y. Kuznetsov, Chapter 4 - Corrosion Inhibitors in Cooling Water Systems, in: Z. Amjad, K.D. Demadis (Eds.), Mineral Scales and Deposits, Elsevier, Amsterdam, (2015)85
13. K. Rahmani, R. Jadidian and S. Haghtalab, *Desalination*, 393 (2016) 174
14. F.M. Mahgoub, B.A. Abdel-Nabey and Y.A. El-Samadisy, *Mater. Chem. Phys.*, 120(1) (2010) 104
15. Y.H. Lei, N. Sheng, A. Hyono, M. Ueda and T. Ohtsuka, *Prog. Org. Coat*., 77(2) (2014) 339
16. A. Bellaouchou, B. Kabkab, A. Guenbour and A. Ben Bachir, *Prog. Org. Coat*., 41(1) (2001) 121
17. G.K. Gomma, *Mater. Chem. Phys.*, 55(2) (1998) 131
18. G.K. Gomma, *Mater. Chem. Phys.,* 55(3) (1998) 235
19. S.M. Milić and M.M. Antonijević, *Corros. Sci.*, 51(1) (2009) 28
20. S. Mamaş, T. Kıyak, M. Kabasakaloğlu and A. Koç, *Mater. Chem. Phys.*, 93(1) (2005) 41
21. H.C. Shih and R.J. Tzou, *Corros. Sci.,* 35(1) (1993) 479
22. X. Luo and J. Yu, *Corros. Sci.*, 38(5) (1996) 767
23. M. Finšgar and I. Milošev, *Corros. Sci.*, 52(9) (2010) 2737
24. Y. Zhou, Y. Zuo and B. Lin, *Mater. Chem. Phys.*, 192 (2017) 86
25. J. Turnbull, R. Szukalo, D. Zagidulin and D. Shoesmith, *Corros. Sci.,* 179 (2021) 109147
26. J. Turnbull, R. Szukalo, D. Zagidulin, M. Biesinger and D. Shoesmith, *Mater. Corros.,* 72(1-2) (2021) 348
27. E. Filimonov and A. Shcherbakov, *Prot. Met.,* 40 (2004) 280
28. G. Li, H. Yuan, J. Mou, E. Dai, H. Zhang, Z. Li, Y. Zhao, Y. Dai and X. Zhang, *Compos. Commun.,* 29 (2022) 101043

29. X.G. Zhang, X.Liu, W.P. Dong, E.D. Fan, Z.H. Bai, G.K. Hu, P. Yi, K. Xiao and Y.H. Huang, *Int. J. Electrochem. Sci*., 14 (2019) 2683
30. R. Youda, H. Nishihara, K. Aramaki, *Electrochim. Acta.*, 35 (1990) 1011
31. W. Chen, W.W. Xiao, *Int. J. Electrochem. Sci*., 17 (2022) 220427
32. I. Danaee, M.N. Khomami and A.A. Attar, *J. Mater. Sci. Technol*., 29(1) (2013) 89
33. I. Danaee and S. Noori, *Int. J. Hydrogen Energy*., 36(19) (2011) 12102
34. Y.X. Qiao, X.Y. Wang, L.L. Yang, X.J. Wang, J. Chen, Z.B. Wang, H.L. Zhou, J.S. Zou and F.H. Wang, *J. Mater. Sci. Technol.*, 107 (2022) 197.
35. Y.B. Tang, X.W. Shen, Z.H. Liu, Y.X. Qiao, L.L. Yang, D.H. Lu, J.S. Zou and J. Xu, *Acta Metall. Sin.*, 58 (2022) 324.
36. J. Yang, Z.B. Wang, Y.X. Qiao and Y.G. Zheng, *Corros. Sci.*, 199 (2022) 110210.
37. A.T. Simonović, Ž.Z. Tasić, M.B. Radovanović, M.B. Petrović Mihajlović and M.M. Antonijević, *ACS Omega*., 5(22) (2020) 12832
38. Ž.Z. Tasić, M.B. Petrović Mihajlović, M.B. Radovanović, A.T. Simonović and M.M. Antonijević, *J. Mol. Struct*., 1159 (2018) 46
39. K. Sabet Bokati, C. Dehghanian and S. Yari, *Corros. Sci.*, 126 (2017) 272
40. K.W. Fang, C.T. Li, S. Dong, D.B. Zhang, X.f. Wu and H.X. Hu, *Scanning*, (2021)6661872
41. E. Zhang, Y. Chen, Y. Tang and J. Wang, *Rare Metal Mat. Eng.*, 40(5) (2011) 769